frontiers in Earth Science

ORIGINAL RESEARCH
published: 15 March 2022
doi: 10.3389/feart.2022.821497

Deep Crustal Structure Beneath the Pamir–Tibetan Plateau: Insights From the Moho Depth and *Vp/Vs* Ratio Variation

Davlatkhudzha Murodov[1,2], *Wang Mi*[1], *Amirkhamza Murodov*[3], *Ilhomjon Oimuhmmadzoda*[2], *Sherzod Abdulov*[2,4] *and Wang Xin*[1]*

[1]Key Laboratory of Western China's Environmental Systems (Ministry of Education), College of Earth and Environmental Sciences, Lanzhou University, Lanzhou, China, [2]Institute of Geology, Earthquake Engineering and Seismology of National Academy of Sciences of Tajikistan, Dushanbe, Tajikistan, [3]Institute of Tibetan Plateau Research, Chinese Academy of Sciences, Beijing, China, [4]Institute of Geology and Geophysics, Chinese Academy of Sciences, Beijing, China

The Cenozoic convergence between India and Asia has created Earth's thickest crust in the Pamir–Tibetan plateau, leading to broadly distributed deformation and extensive crustal shortening; however, the crustal deformation of the high plateau is still poorly constrained. The variation of the Moho topography and crustal composition beneath the Pamir–Tibetan plateau has an important correlation with the major tectonic units. In this study, the results of the receiver functions have been reviewed and analyzed to observe variations in the Moho depth and crustal *Vp/Vs* ratio beneath the Pamir–Tibetan plateau. We found a notable SE–NW-oriented deep Moho interface that starts from the southeast of the Tibetan plateau and continues to the eastern Pamir with a northward dipping direction, which may indicate the northern frontier of the decoupled lower crust of northward underthrusting of the Indian plate. In contrast, the deepest Moho beneath the Pamir plateau has a southward dipping direction indicating the southward underthrusting Asian plate. In general, the average crustal *Vp/Vs* ratio is relatively low beneath the South-Central Pamir (~1.70), while it is relatively higher (~1.75) under the Himalaya–Lhasa terrane, suggesting more felsic to intermediate rock composition with locally high values indicating a low-velocity zone, possibly caused by partial melting. Elevated *Vp/Vs* ratios are observed beneath the northern Pamir (>1.77) and Qiangtang and Songpan–Ganze terranes (>1.80), which can be related to the high mafic rock content and upwelling hot materials from the upper mantle. The *Vp/Vs* ratio beneath the Pamir–Tibetan plateau presents complex north–south variations with a relatively low crustal *Vp/Vs* ratio in the south, while it gradually increases toward the north of the Pamir and central-northern Tibet, which is probably caused by the joint effects of the northward underthrusting Indian lower crust and southward subduction of the Asian plate, the low-velocity zones within the mid-upper crust, and substantial crustal shortening and thickening. The low to average crustal *Vp/Vs* ratio throughout the plateau (except the central Tibet) indicates a limited amount of hot materials to support the low crustal channel flow model, instead suggesting that crustal thickening and shortening is the main uplifting mechanism of the Pamir–Tibetan plateau.

Keywords: crustal composition, Vp/Vs ratio, Pamir–Tibetan plateau, crustal structure, continental subduction

OPEN ACCESS

Edited by:
Yunfa Miao,
Northwest Institute of Eco-Environment and Resources (CAS), China

Reviewed by:
Kai Cao,
China University of Geosciences Wuhan, China
Syed Tallataf Shah,
COMSATS University Islamabad, Pakistan

***Correspondence:**
Wang Xin
xinw@lzu.edu.cn

Specialty section:
This article was submitted to Structural Geology and Tectonics, a section of the journal Frontiers in Earth Science

Received: *24 November 2021*
Accepted: *24 February 2022*
Published: *15 March 2022*

Citation:
Murodov D, Mi W, Murodov A, Oimuhmmadzoda I, Abdulov S and Xin W (2022) Deep Crustal Structure Beneath the Pamir–Tibetan Plateau: Insights From the Moho Depth and Vp/Vs Ratio Variation. Front. Earth Sci. 10:821497. doi: 10.3389/feart.2022.821497

INTRODUCTION

Lateral variation of Moho discontinuity, crustal thickness, and bulk composition preserve first-order information in plate tectonic evolution and provide important clues in understanding the structural evolution of the crust and upper mantle. In the past two decades, several international seismic arrays, including TIPAGE (Mechie et al., 2012; Schneider et al., 2013), FERGHANA (Schneider et al., 2013; Feld et al., 2015), TIPTIMON (Kufner et al., 2018), and the East Pamir seismic experiment (Xu et al., 2021), have been carried out within the Pamir and its adjacent region, which allowed to obtain an improved local seismic image of the crust and upper mantle in this region. The results of seismic refraction/wide-angle reflection and P and S receiver functions indicate that the crustal thickness varies from ~58 km beneath the southern Tien Shan to ~74 km under the North Pamir and ~66 km beneath the South Pamir, where it shallows to about ~40 km below the basins surrounding the Pamirs (Mechie et al., 2012; Xu et al., 2021). The CCP stacking images indicate the presence of a Moho offset at the eastern part of the Pamir, which may mark the boundary between the Pamir and the Tarim block, suggesting that pure shear shortening is responsible for the crustal thickening in the northeast of the Pamir (Xu et al., 2021). Furthermore, a Moho doublet with the deeper interface down to a depth of ~90 km has been highlighted beneath the Central Pamir, where the Asian continental lower crust delaminates and rolls back (Schneider et al., 2019). The thick crust and doublet Moho beneath the Pamir plateau may also suggest the crustal stacking and clashing of tectonic units underneath the Pamir plateau.

Likewise, numerous geophysical observations have been carried out to reveal the detailed crustal and upper mantle structures of the Tibetan plateau, including ANTILOPE (Zhao et al., 2010; Xu et al., 2015; Murodov et al., 2018), INDEPTH (Zhao et al., 1993; Yuan et al., 1997; Kind et al., 2002; Kumar et al., 2006), Hi-CLIMB (Nábělek et al., 2009), Sino-American (Owens et al., 1993), Sino-French (Wittlinger et al., 2004). Overall, the receiver function results of these observations suggest that the Moho depth increases from 50 km beneath the Himalayas in the south of the plateau and gradually deepens to ~80–90 km under the Qiangtang terrane and shallows again to the north (Wittlinger et al., 2004; Nábělek et al., 2009; Zhang et al., 2014; Murodov et al., 2018).

Considering that the Pamir–Tibetan plateau is composed of a complex amalgamation of Gondwanan crustal fragments that have experienced extensive and widespread tectonic deformation since the Mesozoic, the crustal temperature and composition vary throughout the plateau, which leads to high *Vp/Vs* ratio variation (Yin and Harrison, 2000; He et al., 2014; Robinson, 2015). The average crustal P velocities beneath the Pamirs vary from ~6.26 to 6.30 km/s which are lower than the global average (Mechie et al., 2012; Sippl et al., 2013). Similarly, the average crustal *Vp/Vs* ratio beneath the Central and South Pamir is relatively low (<1.70), which is also lower than the global average for the continental crust (Zandt and Ammon, 1995), suggesting that the crust is predominantly composed of felsic rocks, presumably the result of delamination of the mafic rocks of the lower crust (Mechie et al., 2012; Schneider et al., 2019). However, the *Vp/Vs* ratio increases to 1.77 northward, toward the southern Tien Shan (Mechie et al., 2012). The results of receiver functions found an average crustal *Vp/Vs* ratio of ~1.75 beneath the Cenozoic gneiss domes of the Central and South Pamir, which are associated with large-scale crustal extension and exhumation (mainly felsic crust) from 25 to 50 km depth and may suggest a middle crustal low-velocity zone (LVZ) (Schneider et al., 2019). In addition, the velocity model derived by surface wave tomography also imaged an intracrustal LVZ at 20–50 km depth overlain by high-velocity gneiss domes in the southern Pamir, implying the existence of crustal partial molten rocks (Li et al., 2018).

According to the result of receiver function analysis, the *Vp/Vs* ratio beneath southern Tibet is ~1.70, which is lower than the global continental crust average, suggesting that the crust mainly consists of felsic and intermediate rocks without any evidence of partial melt (Nábělek et al., 2009). Under the Lhasa terrane, the *Vp/Vs* ratio is comparatively high, indicating the presence of localized partial melting in the middle and lower crust (Kind et al., 2002). In contrast, it is very high beneath the Qiangtang and Songpan–Ganze terranes, which may be related to joint effects of the more mafic composition and partial melt within the crust (Zhao et al., 2011). In the past decades, the seismic surveys and accumulated seismic data within the Pamir plateau and Tibet plateau have been used separately for various geophysical observations, yet they have not been jointly implemented based on the receiver functions analysis. In this paper, we combine and review previously published receiver function data beneath the Pamir–Tibetan plateau to investigate the Moho topography and crustal *Vp/Vs* ratio variations and their tectonic implications.

OVERVIEW OF TECTONIC SETTINGS

The Pamir–Tibetan plateau has experienced intense tectonic deformation due to the ongoing India–Asia collision that initiated crustal thickening and shortening, resulting in the thickest crust (90 km) on Earth. The Pamir–Tibetan plateau is composed of the same terranes that rifted from Gondwana and subsequently amalgamated on the south margin of Asia prior to the India–Asia collision (Burtman and Molnar, 1993; Yin and Harrison, 2000). However, due to the complex tectonic history, the terranes in the Pamirs have translated northward compared to their counterparts in Tibet. Intracontinental subduction models predict that the structures in the Pamirs have migrated northward by around 300 km with respect to the Himalaya-Tibetan plateau since the Late Cenozoic and that the total amount of crustal shortening that occurred during the Cenozoic is higher in the Pamirs than in Tibet (Burtman and Molnar, 1993; Zubovich et al., 2010). However, recent structural and stratigraphic studies referring to the sedimentary rocks in the Tajik and Tarim basins, which were eroded from the Pamirs during orogenic growth, suggest that the northward movement of the Pamir structures is less than 100 km (Chapman et al., 2017; Chen et al., 2018). The northern Pamir contains the late Paleozoic to early Mesozoic arcs and intervening subduction-accretion

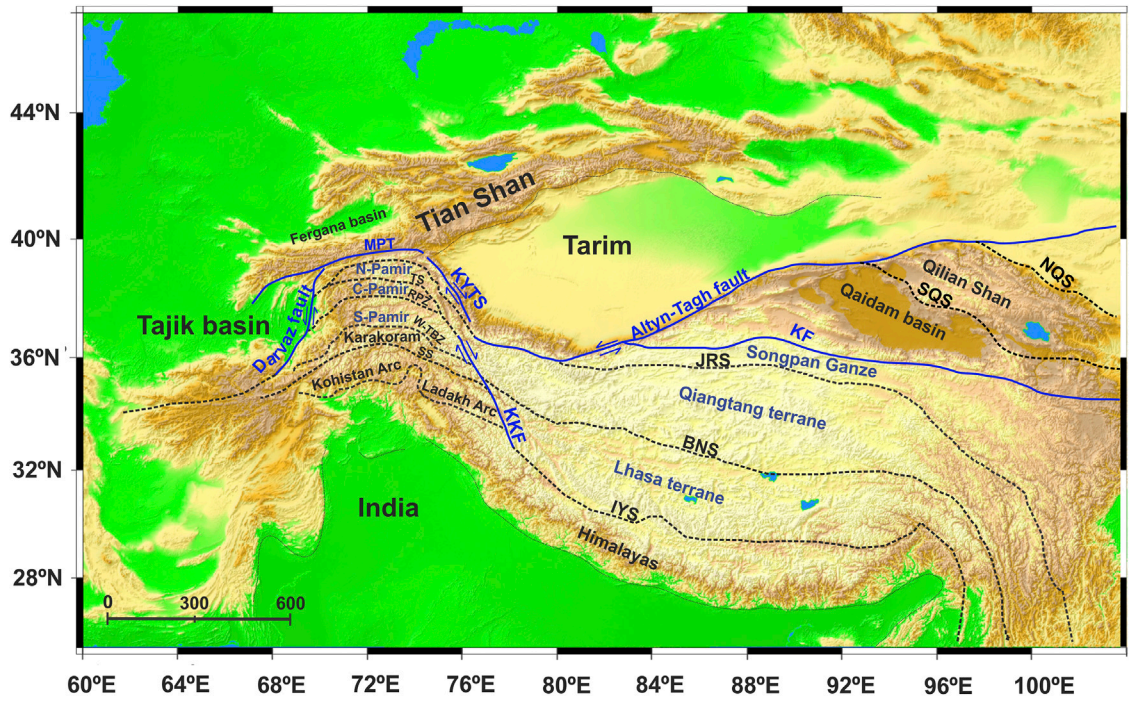

FIGURE 1 | A topographic map of the Pamir–Tibetan plateau and its surrounding regions. The blue colored terranes represent Gondwanan terranes that successively accreted onto the Eurasia plate. The dashed lines highlight the main suture zones: TS, Tanymas Suture; RPZ, Rushan-Pshart Zone; W-TBZ, Wakhan-Tirich Boundary Zone; SS, Shyok Suture; IYS, Indus Yarlung Suture; BNS, Bangong-Nujiang Suture; JRS, Jinsha River Suture; SQS, South Qialian Suture; NQF, North Qilian Fault. The blue lines highlight the major faults within the Pamir–Tibetan plateau, including KF, Kunlun Fault, KKF, Karakorum Fault; KYTS, Kashgar-Yecheng Transfer System; MPT, Main Pamir Thrust, and Darvaz Fault.

systems like the Kunlun arc and Songpan–Ganze terrane, where the central Pamir is composed of Paleozoic–Jurassic rocks similar to the Qiangtang terrane, and the southern Pamir, with Paleozoic–Mesozoic meta-sedimentary rocks, is correlative with the Lhasa terrane (Schwab et al., 2004). With an arcuate shape and a northward convex mountain range, the Pamir plateau has been acting as a rigid indenter, penetrating northward and depressing the Tajik-Yarkand Basin, which used to link today's Tajik-Tarim basins (Burtman and Molnar, 1993; Schwab et al., 2004). The northward displacement has formed several well-developed thrusting and strike-slip faults in the Pamirs, including the sinistral Darvaz strike-slip fault separating the Tajik Basin to the west, the dextral Kashgar-Yecheng Transfer System (KYTS) dividing the Pamir and Tarim Basins to the east, and the Main Pamir Thrust System (MPT) that separates the Alai Valley to the north. The Pamir terranes are divided into three parts: North Pamir, Central Pamir, and South Pamir (**Figure 1**). The North Pamir is separated from the Alai Valley by the Main Pamir Thrust, which has accommodated a substantial part of the current north–south shortening (300 km) (Burtman and Molnar, 1993). The Central and North Pamir terranes are divided by the south-directed Tanymas thrust (Burtman et al., 2013), while the Central Pamir and the South Pamir terranes are separated by the Rushan Pshart suture (Chapman et al., 2017).

Similarly, the terranes of the Tibetan plateau, including the Kunlun, Songpan–Ganzi, Qiangtang, and Lhasa terranes, coherently accreted to the south of Asia before the arrival of the Indian plate and formed the lithosphere of the Tibetan plateau (Molnar and Tapponnier., 1975; Yin and Harrison, 2000). The terranes are separated by the Kunlun fault (KF), Jinsha River suture (JRS), Bangong-Nujiang suture (BNS), and Indus-Yarlung Suture (IS) that are delineated based on ophiolites found along the suture zones (**Figure 1**). During subduction of the dense Indian lithosphere beneath Tibet, its upper crust scrapped off and formed the highest mountain range in the world, the Himalayas, in the south of the Tibetan plateau (Capitanio et al., 2010). While it has been widely accepted by the research community that the Pamir–Tibetan plateau has uplifted in response to the Cenozoic India–Asia convergence, its uplifting mechanism and crustal structure remain poorly constrained.

In terms of deep seismicity, the Pamir–Hindu Kush hosts an intense intermediate-depth seismicity zone that extends down to 250 km (**Figure 2B**) (Koulakov and Sobolev, 2006; Negredo et al., 2007; Sippl et al., 2013; Kufner et al., 2017). The spatial location of the hypocenters of the earthquakes beneath the Pamir and Hindu Kush forms an S-shaped seismic zone, suggesting the presence of two converging subduction zones; a steep northward dipping Indian lithosphere under the Hindu Kush and southward subduction of Asian lithosphere beneath the Pamir (Negredo et al., 2007; Sobel et al., 2013; Kufner et al., 2016). Recent studies

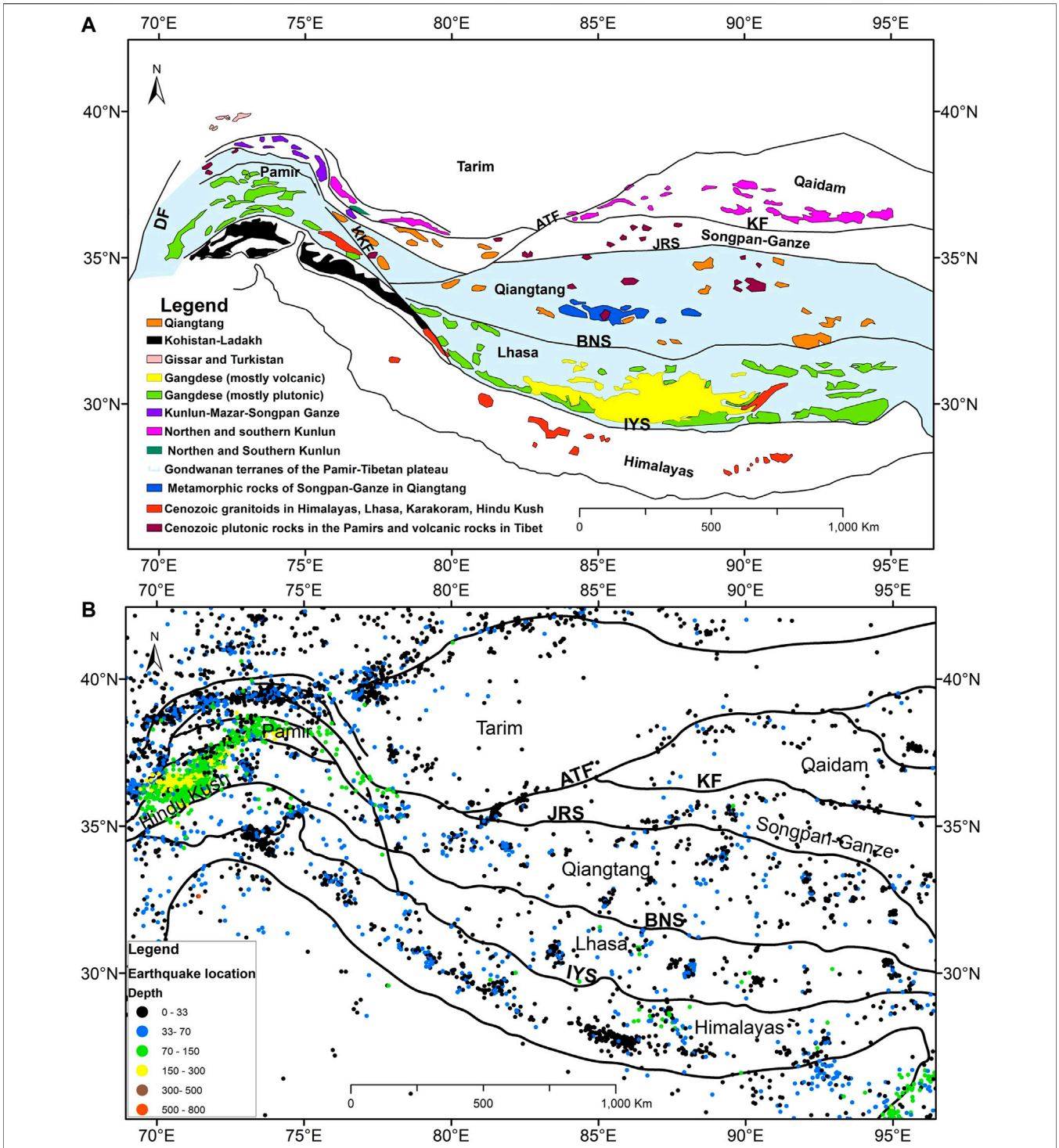

FIGURE 2 | (A) Geological map showing the location of magmatic rocks beneath the Pamir–Tibetan plateau modified after Schwab et al. (2004). **(B)** Map of shallow and intermediate-depth earthquakes beneath the Pamir–Tibetan plateau from time period of 1990–2022 with magnitude >4.5 obtained from Incorporated Research Institutions for Seismology (https://www.iris.edu/hq/).

of the geometry of seismicity constrained by earthquake location and teleseismic tomography show that the Pamir seismic zone forms a curviplanar arc dipping east to the south in the east Pamir and bending to an eastward dip beneath the southwestern Pamir (Sippl et al., 2013; Kufner et al., 2017). Intense intermediate-depth seismicity generated by these north–south contrast high seismic velocity bodies has been interpreted as evidence of ongoing intracontinental subduction (Schneider et al., 2013; Sobel

et al., 2013) or forced delamination (Kufner et al., 2016). However, the different dips of the intermediate-depth seismic zones beneath the Pamir and Hindu Kush invoked various controversial interpretations about the plate configuration, such as the one slab model suggesting a single contorted slab of Indian (Pegler and Das, 1998) or Asian origin (Perry et al., 2019) and the two slab scenario implying two dipping slabs in opposite directions—northward dipping Indian lithosphere beneath the Hindu Kush and southward subduction/delamination Asian slab beneath the Pamir (Burtman and Molnar, 1993; Koulakov and Sobolev, 2006).

In contrast to the Pamir plateau, no distinct deep or intermediate-depth seismic zone is observed beneath the Tibetan plateau. The most supported model for southern Tibet is the Argant-type subduction model (Argand, 1922), where the Indian subcontinent horizontally underthrusts beneath the Tibetan plateau along the Main Boundary Thrust and its upper-crust scrapes off, forming the high Himalayan mountains, and its northward lower crust terminates at the Moho doublet (Kind et al., 2002; Nábělek et al., 2009). Moreover, to quantify the uplift mechanism of the Tibetan plateau, three end-member models have been proposed. 1) Rigid block extrusion model suggests that the deformation is accommodated by a combination of crustal thickening, underthrusting and rigid block motion along large-scale strike-slip faults (Tapponnier et al., 2001). 2) The distributed thickening and shortening model proposed by (England and Houseman, 1986), advocates a vertically coherent deformation across the entire lithosphere, that is, the N-S convergence is largely accommodated by horizontal shortening and vertical thickening. 3) Crustal channel flow explains that the deformation is accommodated by folding and thrusting in the upper crust, supported by lower crust plastic flow (Royden et al., 1997). Each of these models explains the uplifting mechanism of the Tibetan plateau, but controversy remains over the geometry of the underthrusting Indian lithospheric mantle beneath the Tibetan plateau. Seismic images indicate that the Indian lithospheric mantle is underthrusting beneath the Himalaya along the Main Himalayan Thrust and has extended sub-horizontally beneath the Lhasa terrane at ~92° in the east (Shi et al., 2015), whereas its western corner continues to extend to the southwestern corner of the Tarim basin in the west (Wittlinger et al., 2004; Rai et al., 2006).

DATA AND METHODS

We have collected published data on teleseismic receiver functions across the Pamir–Tibetan plateau. The *Vp/Vs* ratio and Moho depth data across the Pamir plateau have been taken from the results of receiver functions along the TIPAGE (Schneider et al., 2019) and East Pamir seismic experiment (Xu et al., 2021). The crustal thickness and *Vp/Vs* ratio data beneath the Tibetan plateau have been obtained from the Hi-CLIMB array (Li J. and Song X., 2021), Namche Barwa Project (Xu et al., 2013), ANTILOPE-I, II, IV (Xu et al., 2015; Xu et al., 2017; Murodov et al., 2018), TW-80 (Zhang et al., 2014), INDEPTH (Yue et al., 2012), and from other temporary and permanent seismic stations throughout Tibet and its adjacent regions (Tian and Zhang, 2013; He et al., 2014; Cheng et al., 2021). The combination of these datasets enables us to correlate the crustal structure of Pamir and Tibet based on the crustal *Vp/Vs* ratio variation. In addition, the joint dataset allows observing the Moho depth beneath the Tibetan plateau and its association with the northern underthrusting Indian plate.

The P-receiver function is a well-established technique that uses a natural earthquake as a source and portable/permanent seismic stations as receivers in order to detect the depth variation of seismic velocity discontinuities beneath a seismic station using the P-to-S (Ps) conversions and associated multiples that originate from discontinuities at different depths. The time difference between the arrival time of the P phase and the converted Ps phase is calculated to determine the converted depth. The main processing steps of the receiver functions include coordinate rotation and deconvolution (Yuan et al., 1997; Kind et al., 2012). The collected Moho depth and *Vp/Vs* ratio values in our review have been calculated by the slant-stack method of (Zhu and Kanamori, 2000), which determines crustal thickness (H) and *Vp/Vs* ratio (κ) by searching for the maximum objective function value in the H-κ domain through a grid search. The algorithm sums the weighted receiver function amplitudes at predicted arrival times for the Ps phase and its multiples for different values of possible crustal thicknesses (H) and *Vp/Vs* ratio (κ).

DISCUSSION

Moho Depth Variation and Its Correlation With Tectonic Units

It is widely assumed that the India–Asia convergence created the vast crustal thickness of the Pamir–Tibetan plateau and the leading uplifting models, including crustal thickening and shortening model, require accurate size, shape, and northern extension of the subducted Indian plate to calculate surface uplift. However, the geometry of Greater India and its northern frontier is still being debated extensively. We traced the deepest Moho interface continuously from the southeast of the Tibetan plateau to the high Pamir mountains derived from receiver functions analysis and revealed its tectonic implications. **Figure 3** displays the results of the Moho abrupt change along the N-S profiles across the Pamir–Tibetan plateau. In the southeast of Tibet along the "Gangdese 92° E" transect, the deepest Moho depth has been found at ~30.8° N–92° E, northern vicinity of the Lhasa terrane (Shi et al., 2015). In the central part of the Tibetan plateau, the seismic data from the INDEPTH project (Kind et al., 2002) revealed the maximum thickness of the crust (78 ± 3 km) with Moho doublet within the Lhasa terrane at ~30° N–92° E. To the west of the INDEPTH profile, receiver function images from the ANTILOPE-II seismic array (Xu et al., 2015) and Hi-CLIMB Experiment (Nábělek et al., 2009) depicted the deepest Moho with a Moho doublet and a step-rise Moho at ~33° N–85°. In the western part of Tibet, P and S receiver functions imaged along the north–south profile of ANTILOPE-I (Murodov et al., 2018) and

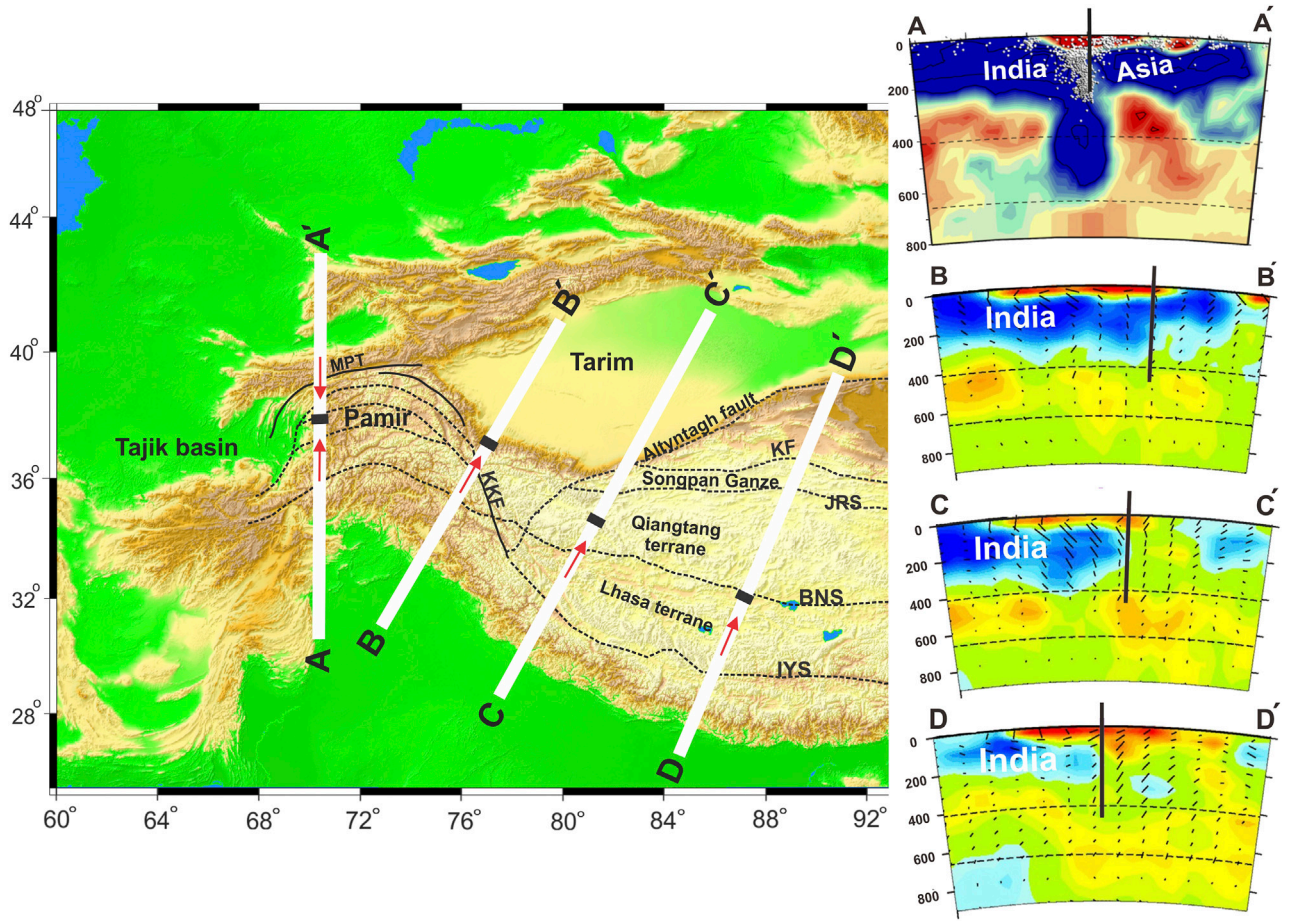

FIGURE 3 | N-S cross-sections tomographic images highlight the Indian lithospheric mantle beneath the Tibetan plateau and the Asian lithospheric mantle beneath the Pamir plateau (Negredo et al., 2007; Wei et al., 2016). The vertical black lines in the cross-sections and black lines along the profiles indicate the location of the northern boundary of the northward underthrusting Indian plate and the southern limit of the Asian plate, where the red arrows represent the subducting/underthrusting directions of the plates.

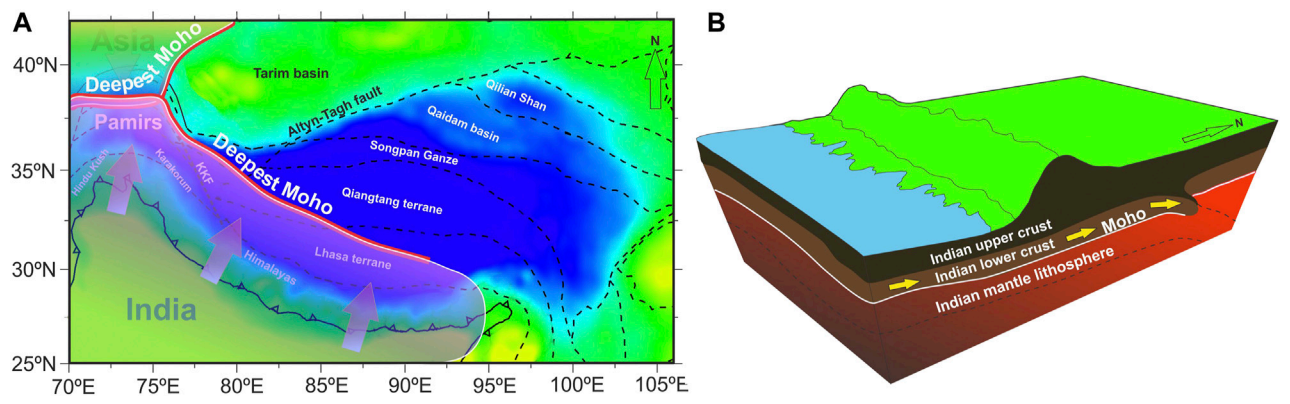

FIGURE 4 | (A) Sketch map showing the deepest Moho interface beneath the Pamir–Tibetan plateau. The bold red lines show the deepest Moho depth with a northward direction interface along the N-S profiles across the Tibetan plateau and a southward direction interface beneath the Pamir plateau. The black dashed lines mark the main tectonic boundaries. **(B)** Cartoon showing the crust and Moho topography, with north dip interface of the Moho discontinuity at the northern margin of Indian lower crust with the deepest Moho forming a synform and step-rise form.

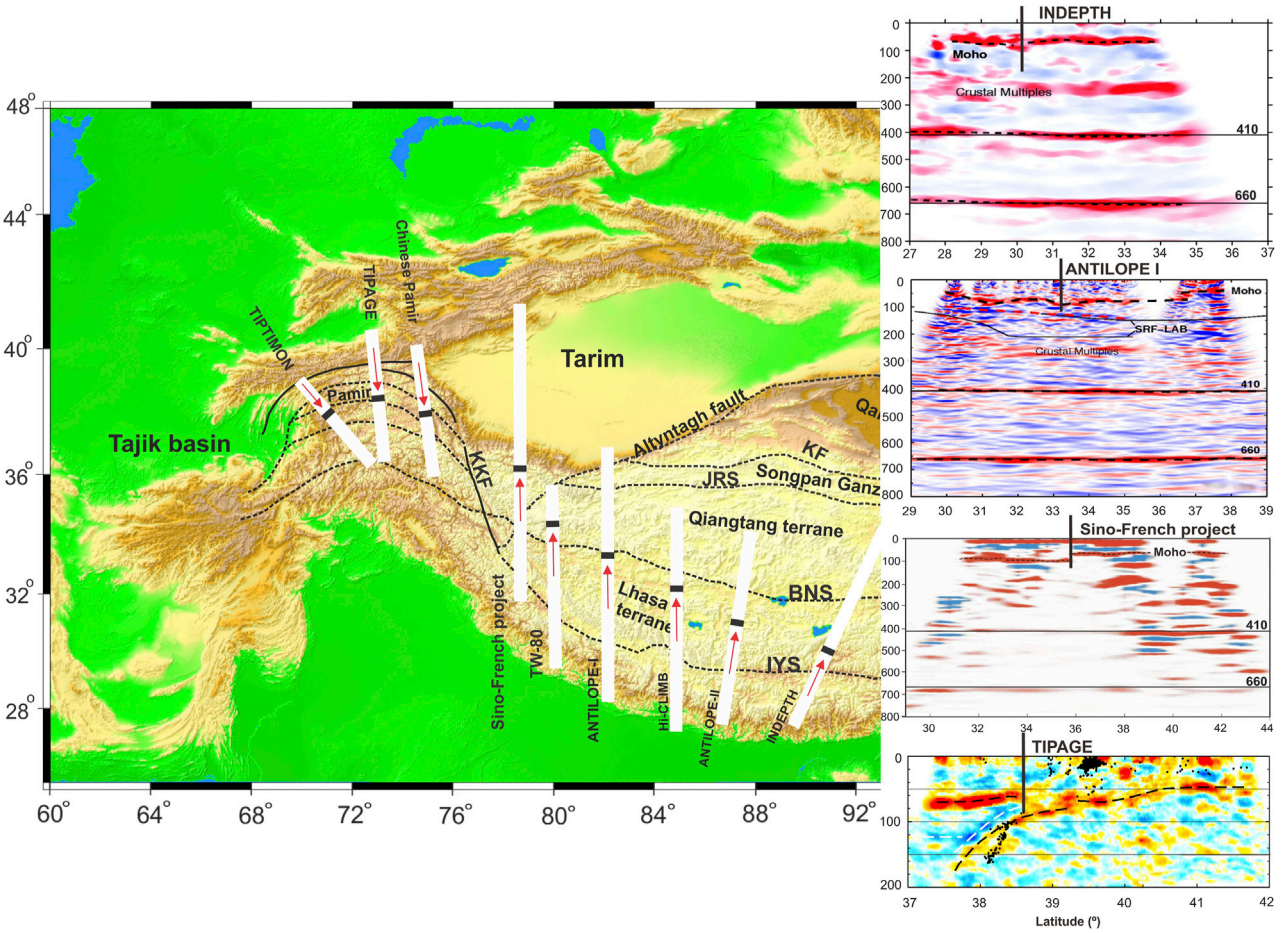

FIGURE 5 | N–S Moho discontinuity derived from receiver functions images beneath the Pamir–Tibetan plateau along INDEPTH (Kind et al., 2002), Hi-CLIMB (Nábělek et al., 2009), ANTILOPE I,II (Zhao et al., 2010), TW-80 (Zhang et al., 2014), Sino-French project (Wittlinger et al., 2004), Chinese Pamir (Xu et al., 2021), TIPAGE (Schneider et al., 2013), and TIPTIMON (Schneider et al., 2019) projects. The vertical black lines in the cross-sections and the black lines along the profiles indicate the northern boundary of the underthrusting Indian plate, where the red arrows show subducting/underthrusting direction of the plates.

the TW-80 experiment (Zhang et al., 2014) imaged the deepest Moho at ~33.7° N–82° E and ~35° N–80° E respectively, which continues with a northward dipping interface. In parallel to the TW-80 and ANTILOPE-I profiles to the west, the teleseismic image from the Sino-French project imaged the maximum crustal thickness (90 km) at ~36.2° N–78° E under the western Qiangtang (Wittlinger et al., 2004). Further west, the deepest Moho is found beneath the eastern Pamir (Xu et al., 2021). It should be noted that from east to west, the observed deepest Moho has a northward gradually dipping interface with an abrupt rise after reaching the maximum depth (**Figure 4B**).

Using a combination of several datasets derived from receiver functions along the INDEPTH profile and its vicinity, (Kumar et al., 2006) suggest that about 500 km of the Indian lithosphere is almost horizontally subducting beneath central Tibet. The horizontal underthrusting Indian plate beneath the Tibetan plateau extends to the location of the deepest Moho found in this study (**Figure 4A**). Northward limit of the Indian plate has also been inferred from elevation, gravity, and geoid anomalies' results, which reach to the location of the deepest Moho observed in this study, agrees well with our interpretation of northward boundary of the northward underthrusting Indian plate (Jiménez-Munt et al., 2008). Furthermore, the results of receiver function analysis conducted by (Rai et al., 2006) in the west of the Tibetan plateau suggest that western Tibet, as far north as the Altyn Tagh, is underlain by Indian plate. The northern frontier of the Indian plate marked in these observations correlates well with the deepest Moho found in our review from east to west. Moreover, the results of P-wave tomography revealed that the horizontal distance over which presumed Indian lithosphere underthrusts beneath Tibet may underlie most of the plateau in the west, where it decreases to the east and shows no indication further than the Indus–Yarlung Suture zone in the east (Li et al., 2008). The leading edge of the Indian plate marked in tomographic observation stretches to the location where the maximum Moho depth is observed in our review (**Figure 5**) (Li et al., 2008; Wei et al., 2016). This is in good agreement with our interpretation of the SE–NW-oriented deepest Moho based on the receiver functions cross-section, which forms a synform with the northern frontier of the

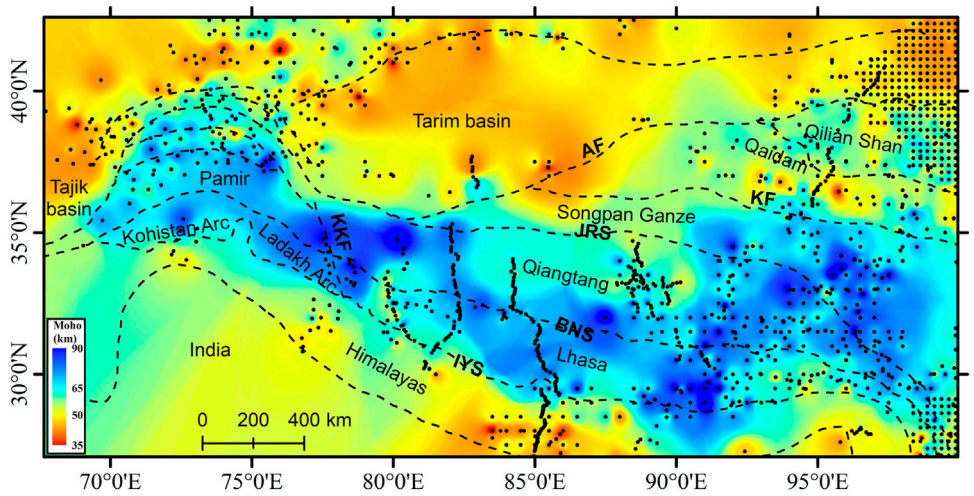

FIGURE 6 | Map of crustal thickness beneath the Pamir–Tibetan plateau. The Moho depth values have been obtained from receiver function analysis conducted across the Pamir and Tibetan plateau. The black circles mark the locations of the seismic stations. AF, Altyn-Tagh Fault; KF, Kunlun Fault; JRS, Jinsha River Suture; IYS, Indus Yarlung Suture; BNS, Bangong-Nujiang Suture; KKF, Karakorum Fault. The crustal thickness values beneath the Pamir plateau have been taken from published data of the TIPAGE (Schneider et al., 2019) and East Pamir seismic experiment (Xu et al., 2021). Beneath the Tibetan plateau, we have used the crustal thickness values derived from the receiver functions along Hi-CLIMB (Li J. and Song X., 2021), Namche Barwa Project (Xu et al., 2013), ANTILOPE-I and II (Xu et al., 2015; Xu et al., 2017; Murodov et al., 2018), TW-80 (Zhang et al., 2014), INDEPTH (Yue et al., 2012), (Tian and Zhang, 2013; He et al., 2014; Cheng et al., 2021).

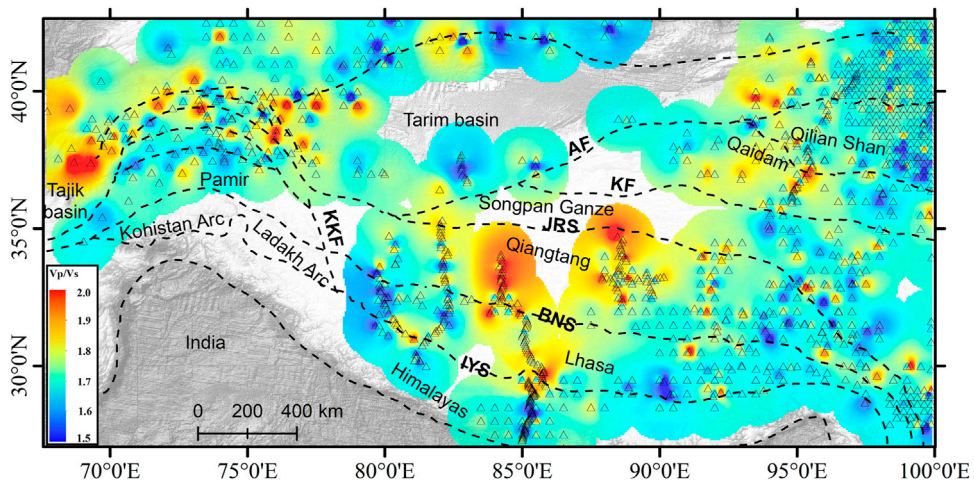

FIGURE 7 | Map of crustal *Vp/Vs* ratio variation beneath the Pamir–Tibetan plateau. The *Vp/Vs* ratio values have been obtained from receiver function analysis conducted across the Pamir and Tibetan plateau. The triangles indicate the locations of the stations. AF, Altyn-Tagh Fault; KF, Kunlun Fault; JRS, Jinsha River Suture; IYS, Indus Yarlung Suture; BNS, Bangong-Nujiang Suture; KKF, Karakorum Fault. The *Vp/Vs* ratio values beneath the Pamir plateau have been taken from published data of the TIPAGE (Schneider et al., 2019) and East Pamir seismic experiment (Xu et al., 2021). Beneath the Tibetan plateau, we have used the *Vp/Vs* ratio values derived from the receiver functions along Hi-CLIMB (Li J. and Song X., 2021), Namche Barwa Project (Xu et al., 2013), ANTILOPE-I and II (Xu et al., 2014; Xu et al., 2017; Murodov et al., 2018), TW-80 (Zhang et al., 2014), INDEPTH (Yue et al., 2012), (Tian and Zhang, 2013; He et al., 2014; Cheng et al., 2021).

Indian plate and supports the interpretation of sub-horizontal underplating of Tibetan crust by Indian crust. We assume that the deepest Moho imaged in the receiver function analysis, continuing from southeast to northwest of the Tibetan plateau, which has a northward dipping interface, indicates the northern limit of lower Indian crust, suggesting that the Indian plate may penetrate as far north as the location of this northward inclined Moho depth (**Figure 3**). We also created the crustal thickness map based on the P receiver functions data and several datasets throughout the Pamir–Tibetan plateau (**Figure 6**). Overall, the bulk crustal thickness in Tibet has more northward expansion in the east, less northward extension in the middle, and again more northward advancement in the west (**Figure 7**). This geometry of crustal thickness agrees well with the Pn tomography results, which suggest that the subducted Indian mantle lithosphere is torn into pieces with different angles and northern limits,

shallower and extending further on the west and east sides, while steeper in the middle (Li and Song, 2018).

In contrast to the Tibetan plateau, the deepest Moho beneath the Pamir plateau has a south-dipping direction (Schneider et al., 2013). The Common Conversion Point (CCP) images from the active source seismic array (Schneider et al., 2013) and seismic refraction/wide-angle reflection data from the passive source seismic array (Mechie et al., 2012) across the Pamirs indicate a clear south-dipping Moho interface, which has been interpreted as the southward subduction of Eurasian continental crust (**Figure 3**). Furthermore, seismic images suggest that the Pamir is almost underlain by nearly horizontal underthrusting Indian mantle lithosphere, which is overlain by the Asian crust (Mechie et al., 2012). A double Moho structure beneath the Central Pamir is observed and interpreted as the result of the westward and northward delamination and rollback of the cratonic Asian lower crust of the Tajik-Tarim Basins beneath the Pamir (Schneider et al., 2019). Moreover, high seismic velocity under the Pamir crust shows the underthrusting Indian lithosphere extending as far north as the Central Pamir (Mechie et al., 2012), and may have replaced the original mantle lithosphere beneath the Pamir (Chapman et al., 2017).

Vp/Vs Ratio Variation and its Tectonic Implication

Poisson's ratio (σ) or *Vp/Vs* ratio, is the ratio of P to S-wave velocity, which can provide important bounds on the composition of the crust. The crustal mineralogy is one of the main factors that induce *Vp/Vs* ratio with only a weak dependence on pressure and temperature (Christensen, 1996). In addition, the *Vp/Vs* ratio can be influenced by the presence of fluid or partial melt, which significantly decreases the shear wave velocity in relation to the compressional wave velocity, leading to a high *Vp/Vs* ratio (Watanabe, 1993). Based on the ratio between P and S wave velocity, the crustal composition is classified to low (σ) (<0.26) (*Vp/Vs* < 1.75), intermediate (σ) (0.26–0.28) and high (σ) (>0.28) (*Vp/Vs* > 1.81) values, whereas the average *Vp/Vs* ratio for a continental crust is estimated to be 1.75–1.77 (Zandt and Ammon, 1995; Christensen, 1996). Felsic composition rocks usually have a low *Vp/Vs* ratio (<1.75), whereas mafic rocks exhibit a relatively high *Vp/Vs* ratio (>1.75). The high amount of quartz (*Vp/Vs* ratio = 1.49) reduces the *Vp/Vs* ratio, while the abundance of plagioclase (*Vp/Vs* = 1.87) increases it.

The Pamirs-Tibetan plateau consist of Paleozoic-Mesozoic volcano sedimentary rocks and the crust experienced Cenozoic high-grade metamorphism and magmatism (**Figure 2A**) (Ding et al., 2003; Schwab et al., 2004). The Central and South Pamir are dominated by clastic and carbonate metasedimentary sequences as well as Paleozoic to Miocene quartzofeldspathic orthogneiss and granitoids (Yin and Harrison, 2000; Schwab et al., 2004). Low crustal *Vp/Vs* ratio (~1.69) has been revealed by seismic refraction/wide-angle reflection beneath the Central and South Pamir suggesting felsic schists and gneisses in the upper part of the lower crust which probably grades into granulite-facies and possibly also eclogite-facies metapelites in the lower part (Mechie et al., 2012). A similar value (<1.70) has been inferred from receiver function analysis (Schneider et al., 2019) and tomography images beneath the Central and South Pamir (Sippl et al., 2013), suggesting a felsic bulk composition that possibly resulted from delamination/founding of the mafic rocks of the lower crust (Kufner et al., 2016). Moreover, a relatively higher crustal *Vp/Vs* ratio (~1.75) has been observed locally beneath the gneiss domes and at mid-crustal level under the Central and South Pamir, which can be a sign of partially molten rocks within the crust (Sippl et al., 2013; Schneider et al., 2019). Furthermore, structural studies suggest that a syn-convergent exhumation occurred along large-scale and normal sense shear zones which exhumed the felsic crust from 25 to 50 km depth in the Central and South Pamir, which led to a low *Vp/Vs* ratio (Rutte et al., 2017). The average *Vp/Vs* ratio increases to ~1.77 toward the North Pamir, South Tien Shan, and beneath the Tajik basin (Mechie et al., 2012; Schneider et al., 2019). Very high crustal *Vp/Vs* ratios (~1.90) have been found along the Main Pamir Thrust, which is probably the result of fluid accumulation within this fault system (Schneider et al., 2019).

In contrast, the average crustal *Vp/Vs* ratio beneath the Himalaya and Lhasa terrane in the southern Tibetan plateau is close to the global average of ~1.75, suggesting more felsic to intermediate rock composition (Murodov et al., 2018). This is slightly higher than those found beneath the Central and South Pamir. The highest *Vp/Vs* ratio (~1.90) is observed beneath the Qiangtang terrane in Central Tibet (Mechie et al., 2004; Yue et al., 2012; liu et al., 2014), pointing toward a widespread occurrence of mafic rocks beneath the Qiangtang and Songpan–Ganzi terranes (**Figure 7**). Moreover, the H-κ stacking results of (He et al., 2014) suggest relatively high *Vp/Vs* ratio anomalies beneath the cenral Tibet which associated it to existence of thermal flow zone within the crust. This is in general agreement with the crustal velocity structure model proposed by (Vergne et al., 2002) in which the Qiangtang Terrane is underlain by a mafic lower crust, which can significantly increase the value of *Vp/Vs* ratio. The high *Vp/Vs* ratio beneath the Qiangtang terrane can also be influenced by widely distributed magmatic rocks that resulted from the northward subducting Lhasa Terrane (Ding et al., 2003; Yue et al., 2012). The Gaussian-Beam migration images of teleseismic P-RFs along the Hi-CLIMB profile suggest that the mafic upper mantle materials have probably been incorporated into the mid to lower crust in Central Tibet during Cenozoic collisions (Nowack et al., 2010). Furthermore, magnetotelluric exploration has shown a high conductivity anomaly in the middle and lower crust beneath the Qiangtang and Songpan–Ganzi terranes, which might be symptomatic of hot materials upwelling from the upper mantle in response to a descending India–Asian lithosphere, which also has a substantial influence on increasing *Vp/Vs* ratio values (Wei et al., 2001; Unsworth et al., 2004). The high *Vp/Vs* ratio beneath the Qaidam basin is related to the thick Cenozoic Qaidam sedimentary layer, which reaches ~15–~20 km (Yin and Harrison, 2000; Unsworth et al., 2004). The average crustal *Vp/Vs* ratio is ~1.75 beneath most of the Tibetan plateau (except Qiangtang terrane), suggesting that the crustal channel flow is not the primary driving force for the uplifting of the Tibetan plateau.

CONCLUSION

We closely observed the deepest Moho imaged by N-S receiver function cross-sections along seismic arrays deployed within the Pamir–Tibetan plateau. The maximum Moho depth with a northward dipping interface from the southeast of Tibet to the southwest of the Tarim basin may indicate the northern limit of the Indian lower crust, suggesting sub-horizontal underthrusting of the Indian plate beneath the Tibetan plateau. In contrast, the deepest Moho beneath Pamir shows a southward dipping interface, indicating a southward underthrusting Asian plate beneath Pamir.

The *Vp/Vs* ratio values vary from low (1.69) beneath the Centeral and South Pamir to average (~1.75) beneath the Himalaya and Lhasa terranes, suggesting felsic to intermediate rock composition, where it increases beneath the North Pamir (~1.80) and Qiangtang to Songpan–Ganze (>1.80) terranes, indicating more mafic materials within the crust or upwelling upper mantle materials. Overall, there is no distinct pattern between the terranes of the Pamir–Tibetan plateau, which is probably due to the fact that the Pamir plateau is located right on the point of India–Asia convergence and has experienced more intense tectonic deformation compared to the Tibetan plateau. Overall, the insignificant amount of high crustal *Vp/Vs* ratio within the plateau suggests that the low crustal channel flow may have contributed to the crustal thickening in the central plateau, but the thickened crust of the plateau presumably resulted from crustal thickening and shortening provoked by the continuous northward movement of the Indian plate relative to stable Eurasia.

DATA AVAILABILITY STATEMENT

The original contributions presented in the study are included in the article/Supplementary Material, further inquiries can be directed to the corresponding authors.

AUTHOR CONTRIBUTIONS

This manuscript was written by DM. XW conceived, designed, and supervised the work. MW modified the figures in the manuscript. The manuscript's English proofreading was done by AM. The data for the manuscript was collected by SA. The manuscript was revised by IO. All authors discussed interpretations and commented on the manuscript.

FUNDING

Financial support for this research was provided by the National Natural Science Foundation of China Grant (Grant No. 42072211), the second Tibetan Plateau Scientific Expedition and Research Program (STEP) (Grant No. 2019QZKK0602), and the open foundation of MOE Key Laboratory of Western China's Environmental Systems (Grant No. lzujbky-2021-kb01).

REFERENCES

Argand, E. (1922). *La tectonique de l'Asie. Conférence faite á Bruxelles, le 10 août 1922, Compte-rendu du XIII*[e] *Congrès géologique international (XIIIe session)-Belgique 1922*, 171–372.

Burtman, V. S., and Molnar, P. (1993). Geological and Geophysical Evidence for Deep Subduction of continental Crust beneath the Pamir. *Geol. Soc. Am. Spec. Pap.* 281, 1–78. doi:10.1130/spe281-p1

Burtman, V. S. (2013). The Geodynamics of the Pamir-Punjab Syntaxis. *Geotecton.* 47, 31–51. doi:10.1134/S0016852113010020

Chapman, J. B., Carrapa, B., Ballato, P., DeCelles, P. G., Worthington, J., Oimahmadov, I., et al. (2017). Intracontinental Subduction beneath the Pamir Mountains: Constraints from Thermokinematic Modeling of Shortening in the Tajik Fold-And-Thrust belt. *Bull. Geol. Soc. Am.* doi:10.1130/B31730.1

Chen, X., Chen, H., Lin, X., Cheng, X., Yang, R., Ding, W., et al. (2018). Arcuate Pamir in the Paleogene? Insights from a Review of Stratigraphy and Sedimentology of the basin Fills in the Foreland of NE Chinese Pamir, Western Tarim Basin. *Earth-Science Rev.* 180, 1–16. doi:10.1016/j.earscirev.2018.03.003

Cheng, S., Xiao, X., Wu, J., Wang, W., Sun, L., Wang, X., et al. (2021). Crustal Thickness and Vp/Vs Variation beneath continental China Revealed by Receiver Function Analysis. *Geophys. J. Int.* 228, 1731–1749. doi:10.1093/gji/ggab433

Christensen, N. I. (1996). Poisson's Ratio and Crustal Seismology. *J. Geophys. Res.* 101, 3139–3156. doi:10.1029/95jb03446

Ding, L., Kapp, P., Zhong, D., and Deng, W. (2003). Cenozoic Volcanism in Tibet: Evidence for a Transition from Oceanic to continental Subduction. *J. Pet.* 44, 1833–1865. doi:10.1093/petrology/egg061

England, P., and Houseman, G. (1986). Finite Strain Calculations of continental Deformation: 2. Comparison with the India-Asia Collision Zone. *J. Geophys. Res.* 91, 3664–3676. doi:10.1029/JB091iB03p03664

Feld, C., Haberland, C., Schurr, B., Sippl, C., Wetzel, H.-U., Roessner, S., et al. (2015). Seismotectonic Study of the Fergana Region (Southern Kyrgyzstan): Distribution and Kinematics of Local Seismicity. *Earth Planet. Sp* 67, 1–13. doi:10.1186/s40623-015-0195-1

He, R., Shang, X., Yu, C., Zhang, H., and Van der Hilst, R. D. (2014). A Unified Map of Moho Depth and Vp/Vs Ratio of continental china by Receiver Function Analysis. *Geophys. J. Int.* 199, 1910–1918. doi:10.1093/gji/ggu365

Jiménez-Munt, I., Fernàndez, M., Vergés, J., and Platt, J. P. (2008). Lithosphere Structure underneath the Tibetan Plateau Inferred from Elevation, Gravity and Geoid Anomalies. *Earth Planet. Sci. Lett.* 267, 276–289. doi:10.1016/j.epsl.2007.11.045

Kind, R., Yuan, X., and Kumar, P. (2012). Seismic Receiver Functions and the Lithosphere-Asthenosphere Boundary. *Tectonophysics* 536-537, 25–43. doi:10.1016/j.tecto.2012.03.005

Kind, R., Yuan, X., Saul, J., Nelson, D., Sobolev, S. V., Mechie, J., et al. (2002). Seismic Images of Crust and Upper Mantle beneath Tibet: Evidence for Eurasian Plate Subduction. *Science* 298, 1219–1221. doi:10.1126/science.1078115

Koulakov, I., and Sobolev, S. V. (2006). A Tomographic Image of Indian Lithosphere Break-Off beneath the Pamir-Hindukush Region. *Geophys. J. Int.* 164, 425–440. doi:10.1111/j.1365-246X.2005.02841.x

Kufner, S.-K., Schurr, B., Haberland, C., Zhang, Y., Saul, J., Ischuk, A., et al. (2017). Zooming into the Hindu Kush Slab Break-Off: A Rare Glimpse on the Terminal Stage of Subduction. *Earth Planet. Sci. Lett.* 461, 127–140. doi:10.1016/j.epsl.2016.12.043

Kufner, S.-K., Schurr, B., Ratschbacher, L., Murodkulov, S., Abdulhameed, S., Ischuk, A., et al. (2018). Seismotectonics of the Tajik Basin and Surrounding Mountain Ranges. *Tectonics* 37, 2404–2424. doi:10.1029/2017TC004812

Kufner, S.-K., Schurr, B., Sippl, C., Yuan, X., Ratschbacher, L., Akbar, A. s. o. M., et al. (2016). Deep India Meets Deep Asia: Lithospheric Indentation, Delamination and Break-Off under Pamir and Hindu Kush (Central Asia). *Earth Planet. Sci. Lett.* 435, 171–184. doi:10.1016/j.epsl.2015.11.046

Kumar, P., Yuan, X., Kind, R., and Ni, J. (2006). Imaging the Colliding Indian and Asian Lithospheric Plates beneath Tibet. *J. Geophys. Res.* 111, a–n. doi:10.1029/2005JB003930

Li, C., van der Hilst, R. D., Meltzer, A. S., and Engdahl, E. R. (2008). Subduction of the Indian Lithosphere beneath the Tibetan Plateau and Burma. *Earth Planet. Sci. Lett.* 274, 157–168. doi:10.1016/j.epsl.2008.07.016

Li, J., and Song, X. (2021). Crustal Structure beneath the Hi-CLIMB Seismic Array in the central-western Tibetan Plateau from the Improved H-κ-C Method. *Earthq Sci.* 34, 1–12. doi:10.29382/eqs-2021-0002

Li, J., and Song, X. (2018). Tearing of Indian Mantle Lithosphere from High-Resolution Seismic Images and its Implications for Lithosphere Coupling in Southern Tibet. *Proc. Natl. Acad. Sci. USA* 115, 8296–8300. doi:10.1073/pnas.1717258115

Li, W., Chen, Y., Yuan, X., Schurr, B., Mechie, J., Oimahmadov, I., et al. (2018). Continental Lithospheric Subduction and Intermediate-Depth Seismicity: Constraints from S-Wave Velocity Structures in the Pamir and Hindu Kush. *Earth Planet. Sci. Lett.* 482, 478–489. doi:10.1016/j.epsl.2017.11.031

Liu, G. C., Shang, X. F., He, R. Z., Gao, R., Zou, C. Q., and Li, W. H. (2014). Topography of Moho beneath the central Qiangtang in North Tibet and its Geodynamic Implication. *Chin. J. Geophys.* 57, 2043–2053. doi:10.6038/cjg20140702

Mechie, J., Sobolev, S. V., Ratschbacher, L., Babeyko, A. Y., Bock, G., Jones, A. G., et al. (2004). Precise Temperature Estimation in the Tibetan Crust from Seismic Detection of the α-β Quartz Transition. *Geol* 32, 601–604. doi:10.1130/G20367.1

Mechie, J., Yuan, X., Schurr, B., Schneider, F., Sippl, C., Ratschbacher, L., et al. (2012). Crustal and Uppermost Mantle Velocity Structure along a Profile across the Pamir and Southern Tien Shan as Derived from Project TIPAGE Wide-Angle Seismic Data. *Geophys. J. Int.* 188, 385–407. doi:10.1111/j.1365-246X.2011.05278.x

Molnar, P., and Tapponnier, P. (1975). Cenozoic Tectonics of Asia: Effects of a Continental Collision: Features of Recent continental Tectonics in Asia Can Be Interpreted as Results of the India-Eurasia Collision. *Science* 189, 419–426. doi:10.1126/science.189.4201.419

Murodov, D., Zhao, J., Xu, Q., Liu, H., and Pei, S. (2018). Complex N-S Variations in Moho Depth and Vp/Vs Ratio beneath the Western Tibetan Plateau as Revealed by Receiver Function Analysis. *Geophys. J. Int.* 214, 895–906. doi:10.1093/gji/ggy170

Nábělek, J., Hetényi, G., Vergne, J., Sapkota, S., Kafle, B., Jiang, M., et al. (2009). Underplating in the Himalaya-Tibet Collision Zone Revealed by the Hi-CLIMB experiment. *Science* 325, 1371–1374. doi:10.1126/science.1167719

Negredo, A. M., Replumaz, A., Villaseñor, A., and Guillot, S. (2007). Modeling the Evolution of continental Subduction Processes in the Pamir-Hindu Kush Region. *Earth Planet. Sci. Lett.* 259, 212–225. doi:10.1016/j.epsl.2007.04.043

Nowack, R. L., Chen, W.-P., and Tseng, T.-L. (2010). Application of Gaussian-Beam Migration to Multiscale Imaging of the Lithosphere beneath the Hi-CLIMB Array in Tibet. *Bull. Seismological Soc. America* 100, 1743–1754. doi:10.1785/0120090207

Owens, T. J., Randall, G. E., Wu, F. T., and Zeng, R. (1993). PASSCAL Instrument Performance during the Tibetan Plateau Passive Seismic experiment. *Bull. Seismol. Soc. Am.* 83, 1959–1970. doi:10.1785/BSSA0830061959

Pegler, G., and Das, S. (1998). An Enhanced Image of the Pamir-Hindu Kush Seismic Zone from Relocated Earthquake Hypocentres. *Geophys. J. Int.* 134, 573–595. doi:10.1046/j.1365-246X.1998.00582.x

Perry, M., Kakar, N., Ischuk, A., Metzger, S., Bendick, R., Molnar, P., et al. (2019). Little Geodetic Evidence for Localized Indian Subduction in the Pamir-Hindu Kush of Central Asia. *Geophys. Res. Lett.* 46, 109–118. doi:10.1029/2018GL080065

Rai, S. S., Priestley, K., Gaur, V. K., Mitra, S., Singh, M. P., and Searle, M. (2006). Configuration of the Indian Moho beneath the NW Himalaya and Ladakh. *Geophys. Res. Lett.* 33. doi:10.1029/2006GL026076

Robinson, A. C. (2015). Mesozoic Tectonics of the Gondwanan Terranes of the Pamir Plateau. *J. Asian Earth Sci.* 102, 170–179. doi:10.1016/j.jseaes.2014.09.012

Royden, L. H., Burchfiel, B. C., King, R. W., Wang, E., Chen, Z., Shen, F., et al. (1997). Surface Deformation and Lower Crustal Flow in Eastern Tibet. *Science* 276, 788–790. doi:10.1126/science.276.5313.788

Rutte, D., Ratschbacher, L., Schneider, S., Stübner, K., Stearns, M. A., Gulzar, M. A., et al. (2017). Building the Pamir-Tibetan Plateau-Crustal Stacking, Extensional Collapse, and Lateral Extrusion in the Central Pamir: 1. Geometry and Kinematics. *Tectonics* 36, 342–384. doi:10.1002/2016tc004293

Schneider, F. M., Yuan, X., Schurr, B., Mechie, J., Sippl, C., Haberland, C., et al. (2013). Seismic Imaging of Subducting continental Lower Crust beneath the Pamir. *Earth Planet. Sci. Lett.* 375, 101–112. doi:10.1016/j.epsl.2013.05.015

Schneider, F. M., Yuan, X., Schurr, B., Mechie, J., Sippl, C., Kufner, S. K., et al. (2019). The Crust in the Pamir: Insights from Receiver Functions. *J. Geophys. Res. Solid Earth* 124, 9313–9331. doi:10.1029/2019JB017765

Schwab, M., Ratschbacher, L., Siebel, W., McWilliams, M., Minaev, V., Lutkov, V., et al. (2004). Assembly of the Pamirs: Age and Origin of Magmatic Belts from the Southern Tien Shan to the Southern Pamirs and Their Relation to Tibet. *Tectonics* 23, a–n. doi:10.1029/2003TC001583

Shi, D., Wu, Z., Klemperer, S. L., Zhao, W., Xue, G., and Su, H. (2015). Receiver Function Imaging of Crustal Suture, Steep Subduction, and Mantle Wedge in the Eastern India-Tibet continental Collision Zone. *Earth Planet. Sci. Lett.* 414, 6–15. doi:10.1016/j.epsl.2014.12.055

Sippl, C., Schurr, B., Tympel, J., Angiboust, S., Mechie, J., Yuan, X., et al. (2013). Deep Burial of Asian continental Crust beneath the Pamir Imaged with Local Earthquake Tomography. *Earth Planet. Sci. Lett.* 384, 165–177. doi:10.1016/j.epsl.2013.10.013

Sobel, E. R., Chen, J., Schoenbohm, L. M., Thiede, R., Stockli, D. F., Sudo, M., et al. (2013). Oceanic-style Subduction Controls Late Cenozoic Deformation of the Northern Pamir Orogen. *Earth Planet. Sci. Lett.* 363, 204–218. doi:10.1016/j.epsl.2012.12.009

Tapponnier, P., Zhiqin, X., Roger, F., Meyer, B., Arnaud, N., Wittlinger, G., et al. (2001). Oblique Stepwise Rise and Growth of the Tibet Plateau. *Science* 294, 1671–1677. doi:10.1126/science.105978

Tian, X., and Zhang, Z. (2013). Bulk Crustal Properties in NE Tibet and Their Implications for Deformation Model. *Gondwana Res.* 24, 548–559. doi:10.1016/j.gr.2012.12.024

Unsworth, M., Wenbo, W., Jones, A. G., Li, S., Bedrosian, P., Booker, J., et al. (2004). Crustal and Upper Mantle Structure of Northern Tibet Imaged with Magnetotelluric Data. *J. Geophys. Res.* 109. doi:10.1029/2002jb002305

Vergne, J., Wittlinger, G., Hui, Q., Tapponnier, P., Poupinet, G., Mei, J., et al. (2002). Seismic Evidence for Stepwise Thickening of the Crust across the NE Tibetan Plateau. *Earth Planet. Sci. Lett.* 203, 25–33. doi:10.1016/S0012-821X(02)00853-1

Watanabe, T. (1993). Effects of Water and Melt on Seismic Velocities and Their Application to Characterization of Seismic Reflectors. *Geophys. Res. Lett.* 20, 2933–2936. doi:10.1029/93GL03170

Wei, W., Unsworth, M., Jones, A., Booker, J., Tan, H., Nelson, D., et al. (2001). Detection of Widespread Fluids in the Tibetan Crust by Magnetotelluric Studies. *Science* 292, 716–719. doi:10.1126/science.1010580

Wei, W., Zhao, D., Xu, J., Zhou, B., and Shi, Y. (2016). Depth Variations of P-Wave Azimuthal Anisotropy beneath Mainland China. *Sci. Rep.* 6. doi:10.1038/srep29614

Wittlinger, G., Vergne, J., Tapponnier, P., Farra, V., Poupinet, G., Jiang, M., et al. (2004). Teleseismic Imaging of Subducting Lithosphere and Moho Offsets beneath Western Tibet. *Earth Planet. Sci. Lett.* doi:10.1016/S0012-821X(03)00723-4

Xu, Q., Zhao, J., Pei, S., and Liu, H. (2013). Imaging Lithospheric Structure of the Eastern Himalayan Syntaxis: New Insights from Receiver Function Analysis. *J. Geophys. Res. Solid Earth* 118, 2323–2332. doi:10.1002/jgrb.50162

Xu, Q., Zhao, J., Yuan, X., Liu, H., Ju, C., Schurr, B., et al. (2021). Deep Crustal Contact between the Pamir and Tarim Basin Deduced from Receiver Functions. *Geophys. Res. Lett.* 48, e2021GL093271. doi:10.1029/2021GL093271

Xu, Q., Zhao, J., Yuan, X., Liu, H., and Pei, S. (2017). Detailed Configuration of the Underthrusting Indian Lithosphere beneath Western Tibet Revealed by Receiver Function Images. *J. Geophys. Res. Solid Earth* 122, 8257–8269. doi:10.1002/2017JB014490

Xu, Q., Zhao, J., Yuan, X., Liu, H., and Pei, S. (2015). Mapping Crustal Structure beneath Southern Tibet: Seismic Evidence for continental Crustal Underthrusting. *Gondwana Res.* 27, 1487–1493. doi:10.1016/j.gr.2014.01.006

Yin, A., and Harrison, T. M. (2000). Geologic Evolution of the Himalayan-Tibetan Orogen. *Annu. Rev. Earth Planet. Sci.* 28, 211–280. doi:10.1146/annurev.earth.28.1.211

Yuan, X., Ni, J., Kind, R., Mechie, J., and Sandvol, E. (1997). Lithospheric and Upper Mantle Structure of Southern Tibet from a Seismological Passive Source experiment. *J. Geophys. Res.* 102, 27491–27500. doi:10.1029/97jb02379

Yue, H., Chen, Y. J., Sandvol, E., Ni, J., Hearn, T., Zhou, S., et al. (2012). Lithospheric and Upper Mantle Structure of the Northeastern Tibetan Plateau. *J. Geophys. Res.* 117, a–n. doi:10.1029/2011JB008545

Zandt, G., and Ammon, C. J. (1995). Continental Crust Composition Constrained by Measurements of Crustal Poisson's Ratio. *Nature* 374, 152–154. doi:10.1038/374152a0

Zhang, Z., Wang, Y., Houseman, G. A., Xu, T., Wu, Z., Yuan, X., et al. (2014). The Moho beneath Western Tibet: Shear Zones and Eclogitization in the Lower Crust. *Earth Planet. Sci. Lett.* 408, 370–377. doi:10.1016/j.epsl.2014.10.022

Zhao, J., Yuan, X., Liu, H., Kumar, P., Pei, S., Kind, R., et al. (2010). The Boundary between the Indian and Asian Tectonic Plates below Tibet. *Proc. Natl. Acad. Sci.* 107, 11229–11233. doi:10.1073/pnas.1001921107

Zhao, W., Kumar, P., Mechie, J., Kind, R., Meissner, R., Wu, Z., et al. (2011). Tibetan Plate Overriding the Asian Plate in central and Northern Tibet. *Nat. Geosci* 4, 870–873. doi:10.1038/ngeo1309

Zhao, W., Nelson, K. D., Che, J., Quo, J., Lu, D., Wu, C., et al. (1993). Deep Seismic Reflection Evidence for continental Underthrusting beneath Southern Tibet. *Nature* 366, 557–559. doi:10.1038/366557a0

Zhu, L., and Kanamori, H. (2000). Moho Depth Variation in Southern California from Teleseismic Receiver Functions. *J. Geophys. Res.* 105, 2969–2980. doi:10.1029/1999JB900322

Zubovich, A. V., Wang, X.-q., Scherba, Y. G., Schelochkov, G. G., Reilinger, R., Reigber, C., et al. (2010). GPS Velocity Field for the Tien Shan and Surrounding Regions. *Tectonics* 29, a–n. doi:10.1029/2010TC002772

Conflict of Interest: The authors declare that the research was conducted in the absence of any commercial or financial relationships that could be construed as a potential conflict of interest.

Publisher's Note: All claims expressed in this article are solely those of the authors and do not necessarily represent those of their affiliated organizations, or those of the publisher, the editors and the reviewers. Any product that may be evaluated in this article, or claim that may be made by its manufacturer, is not guaranteed or endorsed by the publisher.